

Why do classifier accuracies show linear trends under distribution shift?

Horia Mania Suvrit Sra
Department of Electrical Engineering and Computer Science
Massachusetts Institute of Technology
{hmania, suvrit}@mit.edu

December 30, 2020. Revised: February 22, 2021.

Abstract

Recent studies of generalization in deep learning have observed a puzzling trend: accuracies of models on one data distribution are approximately linear functions of the accuracies on another distribution. We explain this trend under an intuitive assumption on model similarity, which was verified empirically in prior work. More precisely, we assume the probability that two models agree in their predictions is higher than what we can infer from their accuracy levels alone. Then, we show that a linear trend must occur when evaluating models on two distributions unless the size of the distribution shift is large. This work emphasizes the value of understanding model similarity, which can have an impact on the generalization and robustness of classification models.

1 Introduction

An important question that arises when evaluating deep learning models is whether the community has overfit to the test sets of popular datasets. Recent studies address this question by trying to replicate the original data collection pipelines and then evaluate models on the newly collected data [15, 17, 18, 24].

While these studies find no overfitting, some of them inadvertently induce a shift between the distributions of the original and new test sets that leads to a drop in model performance. Recht et al. [17] observe accuracy drops of 3% – 15% on CIFAR-10 [13] and of 11% – 14% on ImageNet [4]. Their observations are summarized in Figure 1, from which one can notice a surprising pattern: Classification accuracies on new data are approximately linear functions of the accuracies on the original data, a phenomenon that has also been observed on question-answering data [15] and other variants of ImageNet [1, 23]. These observations raise the following key questions:

- Q1. Why are classification models approximately collinear when evaluated on two data distributions?*
- Q2. When can one expect this phenomenon to occur?*

Answers to these questions provide insights into improving model robustness because training a model robust to distribution shift would mean training a model that is *not* collinear with models developed previously; it would mean training a model that lies close to the identity lines (black

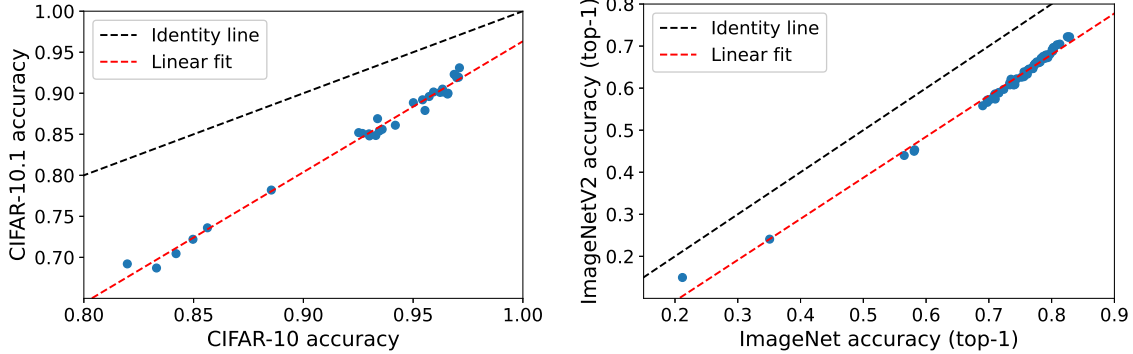


Figure 1: These two figures summarize the findings of Recht et al. [17]. The blue points in the left plot represent 30 CIFAR-10 models evaluated on both the original test set and a new test set, known as CIFAR-10.1. The right plot shows 66 ImageNet models evaluated on both the original validation set and a new test set, known as ImageNetV2. For more examples of distributions shifts, with and without linear trends, one should visit robustness.imagenetv2.org to visualize the testbed developed by Taori et al. [23].

dashed lines) in Figure 1. Therefore, to build robust models it will be helpful to first understand why the models available today are approximately collinear.

While a growing body of work is trying to build robust models [2, 3, 6, 10, 19, 20, 22], as far as we know, there are no models that match human robustness on CIFAR-10.1 and ImageNetV2, the datasets collected by Recht et al. [17] [21, 23]. We hope that understanding when and why models are approximately collinear would inform future work on robust machine learning.

Driven by the above motivation we seek to answer questions **Q1** and **Q2**. We start from a premise inspired by the work of Mania et al. [14] on model similarity. They observe that the probability that two classifiers correctly classify or incorrectly classify a data point is larger than what one would expect if the two classifiers were making predictions independently. We translate this observation into the following assumption: *given two models, the probability that the lower accuracy model classifies a data point correctly while the higher accuracy model classifies it incorrectly is small*. In other words, we assume that high accuracy models correctly classify most of the data points correctly classified by lower accuracy models. Notably, this assumption is satisfied by ImageNet and CIFAR-10 models.

Under this assumption we show that models must be approximately collinear when evaluated on two distributions, unless the size of the distribution shift is large in a certain sense. We also discuss refinements of our analysis that explain why a probit axis scaling leads to an even better linear fit for ImageNet models, as observed by Recht et al. [17].

2 Main results

Let \mathcal{X} be a covariate space and \mathcal{Y} a discrete label space. Let \mathbb{P} and \mathbb{Q} be two probability distributions on $\mathcal{X} \times \mathcal{Y}$. Also, suppose we have a set of h models f_1, f_2, \dots, f_h that map \mathcal{X} to \mathcal{Y} . We are interested in the accuracies

$$\mu_i := \mathbb{E}_{\mathbb{P}} \mathbf{1}(f_i(x) = y), \quad \text{and} \quad \tilde{\mu}_i := \mathbb{E}_{\mathbb{Q}} \mathbf{1}(f_i(x) = y),$$

where the expectations are with respect to the data point $(x, y) \in \mathcal{X} \times \mathcal{Y}$, distributed according to \mathbb{P} and \mathbb{Q} , respectively. Given this notation, our main goal is to show that the accuracies $\{(\mu_i, \tilde{\mu}_i)\}_{i=1}^h$ are approximately collinear, which can be formulated more precisely as follows:

Problem 1. *Under suitable assumptions, show that there exist $\alpha, \beta \in \mathbb{R}$ such that $\tilde{\mu}_i \approx \alpha\mu_i + \beta$ for $1 \leq i \leq h$. Alternatively, given a distribution \mathbb{P} and a set of models f_1, f_2, \dots, f_h , show that for a large class of distribution shifts there exist $\alpha, \beta \in \mathbb{R}$ such that $\tilde{\mu}_i \approx \alpha\mu_i + \beta$ for $1 \leq i \leq h$.*

Our main assumption for Problem 1 is drawn from [14], who observe that the predictions of different image classification models are more similar than one would expect based on accuracies alone. Specifically, if two models f_1 and f_2 with accuracies μ_1 and μ_2 were making mistakes independently of each other, the probability that both models correctly or incorrectly classify a data point would be $\mu_1\mu_2 + (1 - \mu_1)(1 - \mu_2)$. However, they empirically evaluate these similarity probabilities for ImageNet and CIFAR-10 models and observe that model similarities are significantly larger than what the similarities would be if the models were making mistakes independently.

Model similarity is difficult to work with for our purposes because a similarity value can be said to be high or low only in relation to the models' accuracies, which in our analysis vary between 21% and 83%. Instead we work with a more suitable quantity related to model similarity.

Assumption 1. *For any pair of models f_i and f_j with $\mu_i \leq \mu_j$, we have*

$$\mathbb{P}(\{f_i(x) = y\} \cap \{f_j(x) \neq y\}) \leq \zeta.$$

We postpone a discussion of this assumption to Section 3, where we show empirically that most probabilities $\mathbb{P}(\{f_i(x) = y\} \cap \{f_j(x) \neq y\})$ for CIFAR-10 and ImageNet models are less than 0.05. When a set of models satisfies Assumption 1 with $\zeta = 0$ we call it *ordered*, and if a pair of models f_i, f_j satisfies Assumption 1 with $\zeta = 0$, we say that f_j *dominates* f_i . More generally, we call $\mathbb{P}(\{f_i(x) = y\} \cap \{f_j(x) \neq y\})$ the *dominance probability*.

Regardless of ζ , Assumption 1 by itself is insufficient to guarantee that classification accuracies lie close to a line. In fact, in Section 2.2 we show that even when $\zeta = 0$ and Assumption 1 holds for both \mathbb{P} and \mathbb{Q} , there still exist models that are *not* approximately collinear. To ensure collinearity, we need another ingredient, namely, suitable closeness of the distributions \mathbb{P} and \mathbb{Q} ; we present our notion below.

2.1 Characterizing distributional closeness

Various notions of distance between distributions exist, each suitable for different applications [5]. One of the most well-known distances is the total variation: $\text{TV}(\mathbb{P}, \mathbb{Q}) = \sup_A |\mathbb{P}(A) - \mathbb{Q}(A)|$, where the supremum is taken with respect to all measurable events. This distance is stringent because it requires $|\mathbb{P}(A) - \mathbb{Q}(A)|$ to be small for all A . However, for our analysis it suffices to measure $|\mathbb{P}(A) - \mathbb{Q}(A)|$ for only $6\binom{h}{3}$ events that depend on the set $\{f_1, f_2, \dots, f_h\}$ of models.

To see why $6\binom{h}{3}$ events suffice, we first need some notation. For a model f_i let A_i^+ denote the subset of $\mathcal{X} \times \mathcal{Y}$ on which f_i is correct, and A_i^- the subset on which f_i is incorrect. Now we are ready to introduce our notion of closeness.

Definition 1. *We say \mathbb{P} and \mathbb{Q} are $(\delta_1, \delta_2, \nu_1, \nu_2)$ -close if for all distinct $i, j, k \in \{1, 2, \dots, h\}$ and $(\varepsilon_i, \varepsilon_j, \varepsilon_k) \in \{-, +\}^3$, different from $(-, -, -)$ and $(+, +, +)$, we have*

$$-\nu_1 + (1 - \delta_1)\mathbb{P}(A_i^{\varepsilon_i} \cap A_j^{\varepsilon_j} \cap A_k^{\varepsilon_k}) \leq \mathbb{Q}(A_i^{\varepsilon_i} \cap A_j^{\varepsilon_j} \cap A_k^{\varepsilon_k}) \leq \nu_2 + (1 + \delta_2)\mathbb{P}(A_i^{\varepsilon_i} \cap A_j^{\varepsilon_j} \cap A_k^{\varepsilon_k}). \quad (1)$$

In Section 4 we provide empirical motivation for this definition and a more detailed discussion. For now we make a few remarks. Since (1) imposes constraints on the probabilities $\mathbb{Q}(A)$ only for $6\binom{h}{3}$ events A , the distance between \mathbb{Q} and \mathbb{P} is allowed to be large when measured using traditional distances such as TV or KL. In fact, the smaller the number of events A for which $|\mathbb{P}(A) - \mathbb{Q}(A)|$ has to be small the easier it is for \mathbb{P} and \mathbb{Q} to be close.

Also, \mathbb{P} and \mathbb{Q} being $(\delta_1, \delta_2, \nu_1, \nu_2)$ -close does not guarantee by itself that the models f_1, f_2, \dots, f_h are approximately collinear, unless $\delta_1, \delta_2, \nu_1$ and ν_2 are much smaller than the values we observe in practice. In Section 4 we show that the empirical distributions of ImageNet and ImageNetV2 are $(0.31, 0.38, 0.005, 0.008)$ -close, and in Section 2.2 we show that it is possible to have three classification models and two distributions that are $(0.31, 0.38, 0.005, 0.008)$ -close but the three models are far from collinear.

While neither Assumption 1 nor $(\delta_1, \delta_2, \nu_1, \nu_2)$ -closeness is sufficient to guarantee that models are approximately collinear, we show that together they are sufficient. The main idea of our solution to Problem 1 is to look at any three models f_i, f_j , and f_k with accuracies $\mu_i \leq \mu_j \leq \mu_k$, and to consider the line ℓ determined by the points $(\mu_i, \tilde{\mu}_i)$ and $(\mu_k, \tilde{\mu}_k)$. Then, we upper bound the residual from $(\mu_j, \tilde{\mu}_j)$ to the line ℓ , i.e., we upper bound $|\ell(\mu_j) - \tilde{\mu}_j|$. The next result encapsulates our analysis.

Proposition 1. *Let f_1, f_2, \dots, f_h be an ordered set of models and \mathbb{P}, \mathbb{Q} two distributions that are $(\delta_1, \delta_2, \nu_1, \nu_2)$ close. Then, for any three models f_i, f_j, f_k with $\mu_i \leq \mu_j \leq \mu_k$, if ℓ is the line defined by the points $(\mu_i, \tilde{\mu}_i)$ and $(\mu_k, \tilde{\mu}_k)$ and r is the residual $|\ell(\mu_j) - \tilde{\mu}_j|$, we have*

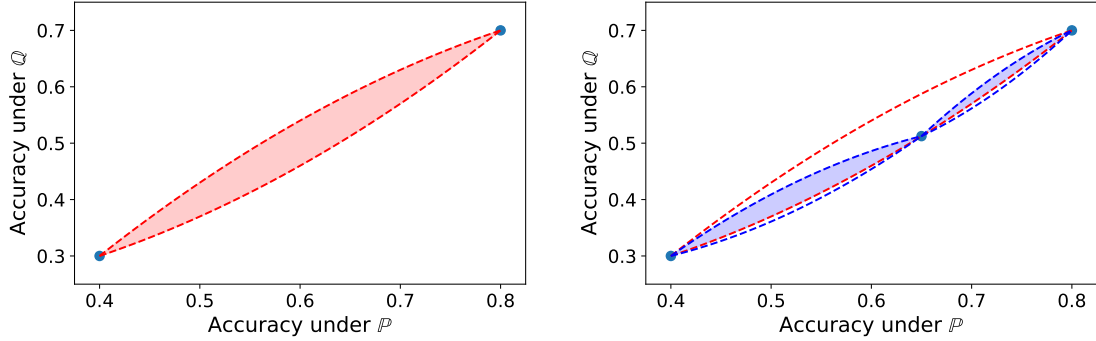
$$r \leq \frac{\delta_1 + \delta_2}{2} \frac{2(\mu_k - \mu_j)(\mu_j - \mu_i)}{\mu_k - \mu_i} + \max\{\nu_1, \nu_2\} + \left(1 + \frac{\max\{\mu_k - \mu_j, \mu_j - \mu_i\}}{\mu_k - \mu_i}\right) \nu_2. \quad (2)$$

Moreover, for any three models there exists a line ℓ' such that all three residuals are equal to $r' = r/2$.

The main takeaway of this result is that given an ordered set of models f_1, f_2, \dots, f_h with respect to a distribution \mathbb{P} , the models are guaranteed to be approximately collinear when evaluated on a distribution \mathbb{Q} , unless the distribution shift between \mathbb{P} and \mathbb{Q} is large in the sense of (1).

Notice that the second factor in the first term of (2) is the harmonic mean of $\mu_k - \mu_j$ and $\mu_j - \mu_i$. To gain intuition about this bound, Figure 2a depicts its guarantee for three ordered models when $\delta_1 = \delta_2 = 0.2$ and $\nu_1 = \nu_2 = 0$. More concretely, we consider two hypothetical models f_i and f_k with $(\mu_i, \tilde{\mu}_i) = (0.4, 0.3)$ and $(\mu_k, \tilde{\mu}_k) = (0.8, 0.7)$. Then, Proposition 1 ensures that any other model f_j that dominates f_i and is dominated by f_k must lie in the red shaded region of Figure 2a. Therefore, if we were to draw the line defined by the two blue points, all other models in the ordered set would lie close to it.

Moreover, (2) applies to any subset of three models. Figure 2b shows what kind of guarantee we can obtain when we take advantage of this fact. Suppose f_j is the middle blue point shown in Figure 2b. Then, by applying (2) two more times we see that a fourth model would have to lie in the smaller blue shaded region. Figure 2b shows that in cases when a linear fit produces residuals that are larger than desired, one can expect to see a much better fit when using piecewise linear regression with two pieces. We come back to this point in Section 5.3, when we discuss why using probit scaling for plotting the ImageNetV2 accuracies as a function of ImageNet accuracies improves the linear fit.



(a) Guarantee after applying (2) once.

(b) Guarantee after applying (2) thrice.

Figure 2: A depiction of bound (2). The blue points represent hypothetical models. Any other models must lie inside the shaded regions when the following conditions hold: the two distributions are $(0.2, 0.2, 0.0, 0.0)$ -close and the set of models is ordered.

Proposition 1 is the core of our answer to Problem 1. It shows that any three models must be approximately collinear when the set of models is ordered and the distribution shift is not too large, as measured by (1). The next corollary shows that all models must be approximately collinear; the proof is deferred to Appendix B.

Corollary 1. *Let f_1, f_2, \dots, f_h be an ordered set of models and \mathbb{P}, \mathbb{Q} be two distributions that are $(\delta_1, \delta_2, \nu_1, \nu_2)$ -close. Then, there exists a line such that the residual from any point $(\mu_i, \tilde{\mu}_i)$ to it is at most*

$$\frac{25}{64}(\mu_h - \mu_1) \frac{\delta_1 + \delta_2}{2} + 3 \max\{\nu_1, \nu_2\}. \quad (3)$$

As expected, this result says that the smaller the distribution shift is (i.e., small $\delta_1, \delta_2, \nu_1$, and ν_2), the closer to a line the models will be. Moreover, the upper bound on the residual depends on the maximum accuracy difference between models in the set. Therefore, if we partition the models into two or more sets, we can get a tighter guarantees on the residuals of a piecewise linear fit.

2.2 Examples and Notation

In this section we show that neither Assumption 1 nor the $(\delta_1, \delta_2, \nu_1, \nu_2)$ -closeness of \mathbb{P} and \mathbb{Q} is alone sufficient to guarantee that models are approximately collinear.

We introduce some notation that is also used in subsequent sections. Given f_1, f_2 , and f_3 we denote the probabilities

$$\begin{aligned} p_{123} &= \mathbb{P}(A_1^+ \cap A_2^+ \cap A_3^+), \\ p_{23} &= \mathbb{P}(A_1^- \cap A_2^+ \cap A_3^+), \\ p_3 &= \mathbb{P}(A_1^- \cap A_2^- \cap A_3^+). \end{aligned}$$

In words, p_{123} is the probability that all three models f_1, f_2 , and f_3 classify a data point sampled from \mathbb{P} correctly. The term p_{23} is the probability that models f_2 and f_3 classify a data point correctly

while f_1 classifies it incorrectly. We also need to consider the probabilities:

$$\begin{aligned} p_1 &= \mathbb{P}(A_1^+ \cap A_2^- \cap A_3^-), & p_{12} &= \mathbb{P}(A_1^+ \cap A_2^+ \cap A_3^-), \\ p_2 &= \mathbb{P}(A_1^- \cap A_2^+ \cap A_3^-), & p_{13} &= \mathbb{P}(A_1^+ \cap A_2^- \cap A_3^+). \end{aligned}$$

These four probabilities are zero when f_1 , f_2 , and f_3 are ordered. Therefore, under the ordering assumption, we have

$$\mu_1 = p_{123}, \quad \mu_2 = p_{123} + p_{23}, \quad \mu_3 = p_{123} + p_{23} + p_3.$$

We use q_{123} , q_{12} , q_1 and so on to denote the analogous probabilities under \mathbb{Q} . Note that although p_1 is zero, q_1 can be nonzero. When the set of models is ordered and the distributions \mathbb{P} and \mathbb{Q} are $(\delta_1, \delta_2, \nu_1, \nu_2)$ -close we know that q_1 , q_2 , q_{12} , and q_{13} are at most ν_2 .

Example 1. We show that there exist models f_1 , f_2 , and f_3 that are ordered with respect to both \mathbb{P} and \mathbb{Q} , but that are not approximately collinear. We emphasize that in this example the models are ordered with respect to both \mathbb{P} and \mathbb{Q} , which is a stronger requirement than that of Assumption 1. Regardless, this requirement is still insufficient to guarantee approximate collinearity of the models.

Since the events $A_1^{\epsilon_1} \cap A_2^{\epsilon_2} \cap A_3^{\epsilon_3}$ are disjoint, there exist models f_1 , f_2 , f_3 and distributions \mathbb{P} and \mathbb{Q} such that these events have any probabilities we wish. We choose

$$\begin{aligned} p_{123} &= 0.6, & p_{23} &= 0.1, & p_3 &= 0.1 \\ p_1 &= p_2 = p_{12} = p_{13} &= 0. \end{aligned}$$

With this choice the models f_1 , f_2 , f_3 have accuracies 0.6, 0.7, and 0.8 and three models are ordered.

Now, we can choose the values of the probabilities of the same events under \mathbb{Q} . Since we want the models to be ordered with respect to \mathbb{Q} too, we set $q_1 = q_2 = q_{12} = q_{13} = 0$. However, without any constraint on the shift between \mathbb{P} and \mathbb{Q} we can set q_{123} , q_{23} , and q_3 to be any nonnegative values whose sum is smaller or equal than one. For example, we can choose $q_{123} = 0.5$, $q_{23} = 0.4$, and $q_3 = 0$, which implies that f_1 , f_2 , and f_3 have accuracies 0.5, 0.9 and 0.9 under \mathbb{Q} . Therefore, the residual of f_2 from the line defined by f_1 and f_3 is 0.2. This residual could be made even larger with a different choice of \mathbb{P} and \mathbb{Q} . The takeaway from this example is that Assumption 1 by itself does not guarantee approximate collinearity even when it holds with respect to both \mathbb{P} and \mathbb{Q} . To avoid such a situation \mathbb{P} and \mathbb{Q} must be sufficiently close in some sense.

Example 2. The perceptive reader will notice that when \mathbb{P} and \mathbb{Q} are $(0, 0, 0, 0)$ -close the models must be collinear. However, in Section 4 we show that ImageNet and ImageNetV2 are $(0.31, 0.38, 0.005, 0.008)$ -close. In this example we show that for such a distribution shift there exist f_1 , f_2 , and f_3 that are far from being collinear. The main message of our analysis is that this situation *cannot* occur when the models are ordered.

We consider models f_1 , f_2 , and f_3 with accuracies $\mu_1 = 0.6$, $\mu_2 = 0.7$, and $\mu_3 = 0.8$. Then, we choose the probabilities of the events $A_1^{\epsilon_1} \cap A_2^{\epsilon_2} \cap A_3^{\epsilon_3}$ as if the models were making predictions independently:

$$\begin{aligned} p_{123} &= \mu_1 \mu_2 \mu_3 = 0.336, \\ p_1 &= \mu_1 (1 - \mu_2)(1 - \mu_3) = 0.036, \\ p_{23} &= (1 - \mu_1) \mu_2 \mu_3 = 0.224, \end{aligned}$$

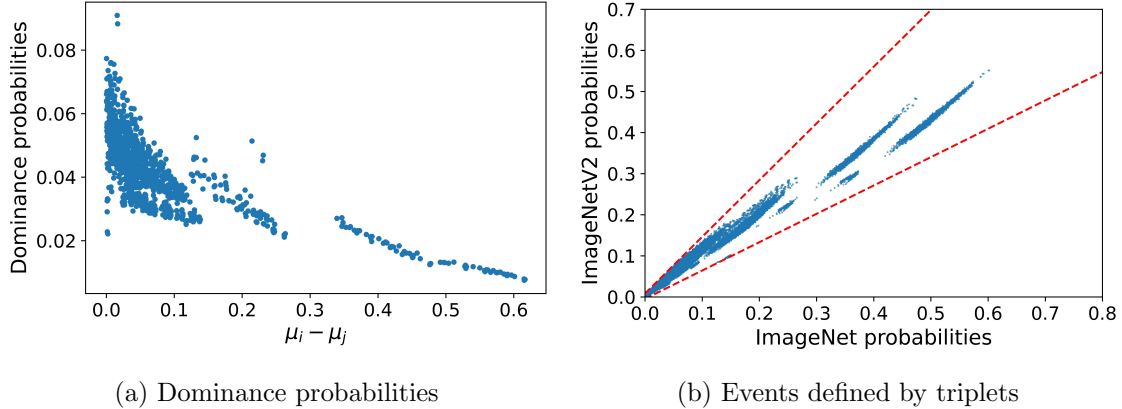


Figure 3: Figure 3a shows the dominance probabilities for all pairs of models. Figure 3b shows 274,560 blue points representing the probabilities of the events $A_i^{\varepsilon_i} \cap A_j^{\varepsilon_j} \cap A_k^{\varepsilon_k}$. The red dotted lines are upper and lower bounds, as in (1), with parameters: $\delta_1 = 0.31$, $\delta_2 = 0.38$, $\nu_1 = 0.005$, and $\nu_2 = 0.008$.

and $p_{12} = 0.084$, $p_{13} = 0.144$, $p_2 = 0.056$, and $p_3 = 0.096$. These models are not ordered because the dominance probabilities are $p_1 + p_{13} = 0.18$, $p_1 + p_{12} = 0.12$, and $p_2 + p_{12} = 0.14$. Therefore, Assumption 1 is satisfied only if $\zeta \geq 0.18$, which is twice as large as the value needed for ImageNet models (see Section 5.1).

Now, if we choose $q_{123} = 0.336$, $q_{12} = 0.053$, $q_{13} = 0.2$, $q_{23} = 0.15$, $q_1 = 0.057$, $q_2 = 0.034$, and $q_3 = 0.14$, we get a distribution \mathbb{Q} that is $(0.31, 0.38, 0.005, 0.008)$ -close to \mathbb{P} . Under \mathbb{Q} the models f_1 , f_2 , and f_3 have accuracies 0.646, 0.573, and 0.826, which means that the residual of f_2 is 0.163. On the other hand, if the models were ordered, Proposition 1 would guarantee that the residual is at most 0.055. Therefore, in addition to \mathbb{P} and \mathbb{Q} being close, Assumption 1 on model dominance needs to hold with a small ζ to guarantee that models are approximately collinear.

3 Model dominance

In this section we take a closer look at Assumption 1. Mania et al. [14] observe that image classification models make similar predictions and use this observation to show that one can re-use test sets more times than previously expected without overfitting. They define the similarity between two models f_i and f_j to be $\mathbb{P}(\mathbb{1}\{f_i(x) = y\} = \mathbb{1}\{f_j(x) = y\})$.

If two models were making mistakes independently of each other, this similarity would be $\mu_i\mu_j + (1 - \mu_i)(1 - \mu_j)$. However, on ImageNet they observed model similarities that are approximately 0.25 higher.

We explained in Section 2 that it is a bit difficult to work with model similarity for our purposes. Instead, given two models f_i and f_j with $\mu_i \leq \mu_j$ we consider the probability that f_i classifies a data point correctly while f_j does not:

$$\mathbb{P}(\{f_i(x) = y\} \cap \{f_j(x) \neq y\}). \quad (4)$$

Recall that we refer to (4) as dominance probability. It is easy to relate the model similarity and

dominance probabilities since the former is equal to

$$1 - (\mu_j - \mu_i) - 2\mathbb{P}(\{f_i(x) = y\} \cap \{f_j(x) \neq y\}).$$

Assumption 1 can be checked empirically. We study $h = 66$ ImageNet models that were collated and evaluated by Recht et al. [17]¹. Figure 3a shows the dominance probabilities of the ImageNet models as a function of their accuracy differences. Note that these probabilities are less than 0.09, and 76% of them are less than 0.05. Also, the dominance probability decreases as the difference in accuracy increases. Hence, it seems that on ImageNet the more accurate a model is the more it dominates lower accuracy models.

4 The size of distribution shift

In this section we discuss the notion of closeness between \mathbb{P} and \mathbb{Q} postulated in Definition 1. Of course, for any distributions \mathbb{P} and \mathbb{Q} there exist parameters $\delta_1, \delta_2, \nu_1$ and ν_2 such that (1) holds. However, this trivial point is not sufficient to justify our assumption. Fortunately, similar notions of closeness between distributions have been used in other contexts. Kpotufe and Martinet [12] used a similar metric to analyze the sample complexity of transfer learning. Coincidentally, inequalities of the form (1) are also used in differential privacy to compare the distributions of outputs of a randomized algorithm applied to two different databases [7, 8, 9].

An important advantage of requirement (1) is that it must hold only for a finite number of events for our analysis to go through. As mentioned in Section 2, the fewer the number of events for which (1) has to hold, the more permissive the notion of closeness between distributions becomes.

Another advantage of requirement (1) is that for the relevant events A , we can estimate $\mathbb{P}(A)$ and $\mathbb{Q}(A)$ on CIFAR-10 and ImageNet and find $\delta_1, \delta_2, \nu_1$, and ν_2 such that (1) holds. Thus, we can estimate the closeness of \mathbb{P} and \mathbb{Q} empirically.

For any data point a model either classifies it correctly or incorrectly. Hence, given three models there are 8 possible correctness outcomes. Definition 1 considers only 6 of the corresponding events. To understand why we do not need to worry about $\mathbb{Q}(A_i^- \cap A_j^- \cap A_k^-)$ and $\mathbb{Q}(A_i^+ \cap A_j^+ \cap A_k^+)$, note that changes in these two probabilities would only move the three points $(\mu_i, \tilde{\mu}_i)$, $(\mu_j, \tilde{\mu}_j)$, and $(\mu_k, \tilde{\mu}_k)$ up or down equally. Therefore, the two probabilities would have no effect on how closely to a line the three points lie.

In Section 2.2 we explained that \mathbb{P} and \mathbb{Q} must be close to guarantee approximate collinearity, but what does it mean for \mathbb{P} and \mathbb{Q} to be far apart? According to Definition 1 there must exist an event among the relevant $6\binom{h}{3}$ events that does not satisfy (1). Nonetheless, our analysis can tolerate some violations of (1). To understand why, suppose we are given four models f_1, f_2, f_3, f_4 , and suppose (1) is satisfied by the events defined by (f_1, f_2, f_4) and (f_1, f_3, f_4) . Then, we can show that f_2 and f_3 lie close to the line defined by f_1 and f_4 , without needing the events defined by the triplets (f_1, f_2, f_3) and (f_2, f_3, f_4) to satisfy (1). Hence, we can guarantee that all models are approximately collinear even when some of the $6\binom{h}{3}$ events do not satisfy (1).

Distributional closeness does not necessarily have to be defined in terms of linear bounds. Instead, our analysis can be performed with bounds of the form $-g_1(\mathbb{P}(A)) \leq \mathbb{Q}(A) - \mathbb{P}(A) \leq g_2(\mathbb{P}(A))$ for some functions g_1 and g_2 . Such a notion of closeness is important in the case of CIFAR-10, since

¹Recht et al. [17] provide 67 models. Even though all 67 models are approximately collinear, we take out one of the three Fisher vector models. We discuss this choice in Appendix C.

for this dataset the linear bounds require large δ_2 and ν_2 , although $|\mathbb{Q}(A) - \mathbb{P}(A)|$ is small for all relevant events. We discuss this point further in Appendix A.

ImageNet and ImageNetV2 are close. We study $h = 66$ ImageNet models that were collated and evaluated by Recht et al. [17]. We would like to find parameters $\delta_1, \delta_2, \nu_1, \nu_2$ such that the bounds in (1) hold for all necessary events defined by triplets of models when the probabilities are evaluated under the ImageNetV2 and ImageNet distributions.

We evaluate these probabilities empirically, which will have some estimation error. Nonetheless, this exercise reveals what are reasonable values of $\delta_1, \delta_2, \nu_1, \nu_2$ so that ImageNet and ImageNetV2 are $(\delta_1, \delta_2, \nu_1, \nu_2)$ -close.

The blue points shown in Figure 3b represent probabilities of the 274,560 events defined by model triplets. All blue points lie in a wedge defined by two lines, with slopes 0.69 and 1.38 and with y -axis intercepts -0.005 and 0.008 respectively. This empirical evaluation suggests that ImageNet and ImageNetV2 are $(0.31, 0.38, 0.005, 0.008)$ -close.

Interestingly, if we only require 95% of the 274,560 points to lie inside the wedge, we can choose $\delta_1 = 0, \delta_2 = 0.25, \nu_1 = 0.005, \text{ and } \nu_2 = 0.005$. Therefore, the vast majority of points lie in a much smaller wedge than the one considered previously. This observation is valuable for Section 5.3, where we discuss the linear fit in probit domain.

5 Main arguments

In Section 5.1 we present the crux of our analysis under the simplifying assumption that the set of models is ordered. Then, in Section 5.2 we discuss what happens when the dominance probabilities are small, but not necessarily zero.

5.1 Proof of Proposition 1

Given an ordered set of models let us consider three models $f_1, f_2, \text{ and } f_3$ with $\mu_1 \leq \mu_2 \leq \mu_3$. Also, let ℓ be the line between the points $(\mu_1, \tilde{\mu}_1)$ and $(\mu_3, \tilde{\mu}_3)$. Then, we upper bound the residual from $(\mu_2, \tilde{\mu}_2)$ to ℓ in the vertical direction (residuals are always measured along the y -axis).

To express this residual we use the notation introduced in Section 2.2. Then, the line ℓ is defined by the equation:

$$\begin{aligned} \ell(\mu) &= \frac{\tilde{\mu}_3 - \tilde{\mu}_1}{\mu_3 - \mu_1}(\mu - \mu_1) + \tilde{\mu}_1 \\ &= \frac{q_{23} + q_3 - q_1 - q_{12}}{p_{23} + p_3}(\mu - p_{123}) + q_{123} + q_{12} + q_{13} + q_1. \end{aligned}$$

Hence, the residual $r := |\ell(\mu_2) - \tilde{\mu}_2|$ is

$$\begin{aligned} r &= \left| \frac{q_{23} + q_3 - q_1 - q_{12}}{p_{23} + p_3} p_{23} + q_{13} + q_1 - q_{23} - q_2 \right| \\ &\leq \left| \frac{q_3 p_{23} - p_3 q_{23}}{p_{23} + p_3} \right| + \left| \frac{p_3}{p_3 + p_{23}} q_1 - \frac{p_{23}}{p_3 + p_{23}} q_{12} + q_{13} - q_2 \right|. \end{aligned} \tag{5}$$

When \mathbb{P} and \mathbb{Q} are $(\delta_1, \delta_2, \nu_1, \nu_2)$ -close we can use the upper and lower bounds (1) on $q_1, q_{13}, q_2, q_{12}, q_3, \text{ and } q_{23}$, which yields the first part of Proposition 1. To show that there is a line ℓ' that halves

the residuals let us denote by A , B , and C the three points $(\mu_1, \tilde{\mu}_1)$, $(\mu_2, \tilde{\mu}_2)$, and $(\mu_3, \tilde{\mu}_3)$. Now, instead of the line ℓ that passes through A and C , we consider the line ℓ' defined by the middles points of the segments AB and BC . Then the residual r' between the three points and ℓ' is equal to $r/2$, gaining a factor of 2 over (2). This argument completes the proof of Proposition 1.

5.2 Approximately ordered models

Now we discuss what happens when the set of models f_1, f_2, \dots, f_h is not ordered, i.e., when the dominance probabilities are allowed to be non-zero. Nevertheless, Figure 3a from Section 3 shows that these probabilities can be assumed to be small (e.g. less than 0.05).

We proceed as in the Section 5.1, using the same notation. Given three models f_1, f_2, f_3 we show that the three points $(\mu_1, \tilde{\mu}_1)$, $(\mu_2, \tilde{\mu}_2)$, and $(\mu_3, \tilde{\mu}_3)$ are approximately collinear. Now, we have $\mu_1 = p_1 + p_{12} + p_{13} + p_{123}$, $\mu_2 = p_2 + p_{12} + p_{23} + p_{123}$, and $\mu_3 = p_3 + p_{13} + p_{23} + p_{123}$. Also, since the set of models satisfies Assumption 1 we know that $p_1 + p_{12}$, $p_1 + p_{13}$, and $p_2 + p_{12}$ are at most ζ .

As before, we consider the line ℓ defined by $(\mu_2, \tilde{\mu}_2)$ and $(\mu_3, \tilde{\mu}_3)$:

$$\ell(\mu) = \frac{\tilde{\mu}_3 - \tilde{\mu}_2}{\mu_3 - \mu_2}(\mu - \mu_2) + \tilde{\mu}_2.$$

Therefore, the residual r from $(\mu_1, \tilde{\mu}_1)$ to ℓ is

$$r = \left| \frac{q_3 + q_{23} - q_1 - q_{12}}{p_3 + p_{23} - p_1 - p_{12}}(p_2 + p_{23} - p_1 - p_{13}) + q_1 + q_{13} - q_2 - q_{23} \right|. \quad (6)$$

Numerical upper bound. Given Assumption 1 and the fact that \mathbb{P} and \mathbb{Q} are $(\delta_1, \delta_2, \nu_1, \nu_2)$ -close, to get the best possible upper bound on (6), one would have to consider many cases, which are determined by the signs of various quantities inside the absolute value. Instead, we compute an upper bound on (6) numerically.

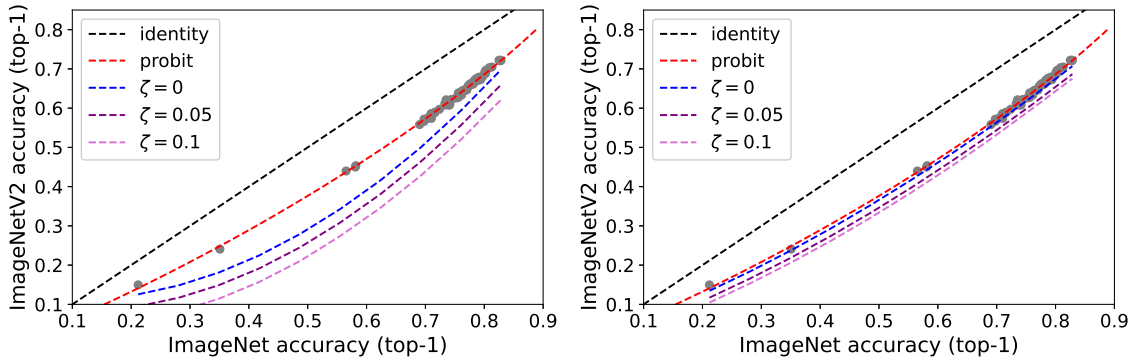
Given three models f_1, f_2, f_3 that satisfy Assumption 1 we compute numerically an upper bound on the residual from f_2 to the line defined by the other two models. To achieve this we grid over the six probabilities of $p_1, p_2, p_3, p_{12}, p_{13}, p_{23}$. To ensure that Assumption 1 holds and to ensure that the models have the desired accuracies we impose the following constraints: $p_1 + p_{12} \leq \zeta$, $p_1 + p_{13} \leq \zeta$, $p_2 + p_{12} \leq \zeta$, and

$$\begin{aligned} p_2 + p_{23} - p_1 - p_{13} &= \mu_2 - \mu_1, \\ p_3 + p_{13} - p_2 - p_{12} &= \mu_3 - \mu_2. \end{aligned}$$

These two conditions ensure that we can choose p_{123} so that the models have the desired accuracies.

Once the \mathbb{P} probabilities of the events $A_i^{\varepsilon_i} \cap A_j^{\varepsilon_j} \cap A_k^{\varepsilon_k}$ are fixed, we grid over the \mathbb{Q} probabilities, ensuring that $\max\{0, -\nu_1 + (1 - \delta_1)p\} \leq q \leq \nu_2 + (1 + \delta_2)p$, for all $p \in \{p_1, p_2, p_3, p_{12}, p_{13}, p_{23}\}$ and corresponding q . For each probability we choose five equally-spaced grid points in the relevant interval.

If we set $\delta_1 = 0.31$, $\delta_2 = 0.38$, $\nu_1 = 0.005$, $\nu_2 = 0.008$, $\zeta = 0.05$ and consider models that are 0.6, 0.7, 0.8 accurate, we find that (6) is at most 0.084. Then, by shifting the line ℓ towards $(\mu_2, \tilde{\mu}_2)$ we can halve the residual. Therefore, in the case we are analyzing, there exists a line such that the residuals of the models f_1, f_2 , and f_3 are at most 0.042. If we choose $\delta_1 = 0.0$, $\delta_2 = 0.25$, $\nu_1 = 0.005$, and $\nu_2 = 0.005$, numerical evaluation shows that (6) is at most 0.045, whereby there



(a) Guarantees with $\delta_1 = 0.31$, $\delta_2 = 0.38$ and $\nu_1 = 0.005$, $\nu_2 = 0.008$.

(b) Guarantees with $\delta_1 = 0.0$, $\delta_2 = 0.25$, and $\nu_1 = \nu_2 = 0.005$.

Figure 4: Comparison between probit linear fit of the ImageNet models and our lower bounds on ImageNetV2 accuracies.

exists a line such that the residuals of the three models are at most 0.0225. We also present our numerical bounds in Figures 4a and 4b, where we also vary ζ . These numerical bounds show that the analytical guarantees derived in Proposition 1 and Corollary 1 do not degrade significantly when the set of models is not ordered, but satisfies Assumption 1 with small ζ .

5.3 Discussion of probit axis scaling

Recht et al. [17] show that using a probit axes scaling leads to a better linear fit for ImageNet models. Concretely, they fit a line to the points $(\Phi^{-1}(\mu_i), \Phi^{-1}(\tilde{\mu}_i))$, where Φ is the CDF of the standard normal distribution, and observe a better linear fit than in Figure 1. The standard linear fit, shown on the right of Figure 1, produces a line with a maximum residual of 0.044 and a R^2 of 0.988. On the other hand, the linear fit in probit domain, shown as the red dashed curves in Figures 4a and 4b, yields a maximum residual of 0.01 and a R^2 of 0.998.

Given the goodness of this fit, it is natural to wonder whether there is an underlying reason for it. Recht et al. [17] describe a generative model for the data distributions and models that leads to a linear fit in probit domain. Our assumptions are less restrictive and we use them to explain why it is likely to have a good fit in probit domain.

In Figure 4a, the red dashed curve is obtained by mapping the linear fit in probit domain back to probability space. To understand what our analysis says about this phenomenon we also show the guarantees provided by (2) and (6) as the blue and purple curves when $\delta_1 = 0.31$, $\delta_2 = 0.38$, $\nu_1 = 0.005$, and $\nu_2 = 0.008$ (values that guarantee that ImageNet and ImageNetV2 are $(\delta_1, \delta_2, \nu_1, \nu_2)$ -close). The maximal value of (6) is computed numerically by gridding, as discussed in Section 5.2. Both the blue and purple curves are lower bounds on test accuracies computed on ImageNetV2. The blue curve assumes the set of models is ordered (i.e. $\zeta = 0$). The other two curves uses Assumption 1 with $\zeta = 0.05$ and $\zeta = 0.1$, respectively.

While the blue and purple curves shown in Figure 4a follow loosely the probit (red) curve, they are not tight lower bounds. We can do better. We already discussed that the choice of parameters $\delta_1 = 0.31$, $\delta_2 = 0.38$, $\nu_1 = 0.005$, $\nu_2 = 0.008$ is conservative. If we set $\delta_1 = 0.$, $\delta_2 = 0.25$, and $\nu_1 = \nu_2 = 0.005$, we get tighter bounds that we plot in Figure 4b. Interestingly, the two lower

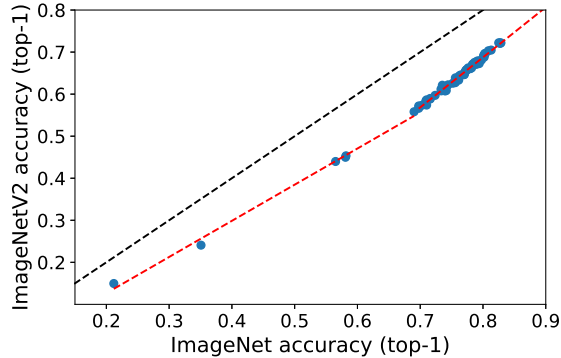


Figure 5: Piecewise linear fit of 66 ImageNet models with two pieces. The switch point between pieces is set to be the 6-th least accurate model.

bounds closely follow the probit curve. Therefore, the goodness of the probit linear fit might be a fortuitous consequence of the models saturating our bounds.

Moreover, we said in Section 2 that when the upper bound (2) is saturated by f_1 , f_h , and some third model f_i , we expect a piecewise linear function to fit the data much better than a simple linear fit. This conclusion can be reached by applying (2) to multiple triplets of models. Indeed, Figure 5 shows a piecewise linear fit with two pieces. The R^2 of this fit is 0.997, which is almost identical to the R^2 of the probit linear fit (the difference between the two R^2 scores is 4×10^{-4}). Observing a good piecewise linear fit is likely to be a more general occurrence than a linear fit in probit domain. In fact, Taori et al. [23] saw that a piecewise linear function fits models fairly well when the models are evaluated on ImageNet-A (a collection of ImageNet test images collected by Hendrycks et al. [11]) and the original ImageNet validation set.

Therefore, while the generative model of Recht et al. [17] shows that models can be exactly collinear in probit domain, our analysis shows that trends that look linear in probit domain occur more generally. Moreover, we saw that a piecewise linear fit with two pieces fits the data equally well. Determining whether a piecewise linear trend occurs more generally than a probit linear trend would be an interesting question for future work to explore.

6 Conclusion

We said that understanding why models are approximately collinear may lead to insights into improving model robustness. According to our analysis, there are roughly three ways in which a new model can be more robust than previous models. In the first case, the linear fit of the previous models has slope larger than one and the new model has higher accuracy than previous models, but it still lies close to the same line. According to terminology introduced by Taori et al. [23], in this situation the new model has *relative robustness*, but does not have *effective robustness* because it is not more robust than what the linear trend predicts.

In the second case, even though the distributions \mathbb{P} and \mathbb{Q} might be $(\delta_1, \delta_2, \nu_1, \nu_2)$ -close with respect to the previous models, the addition of a new model might reveal that the distributions are not close. In this case, some of the relevant events on which the new model classifies correctly can have much higher probabilities under \mathbb{Q} than under \mathbb{P} (i.e. $\mathbb{Q}(A) > \nu_2 + (1 + \delta_2)\mathbb{P}(A)$), making

the new model effectively robust. This situation might occur when the new model is trained on a different dataset than previous models.

Interestingly, the newly released CLIP model, developed by Radford et al. [16] to showcase the power of natural language supervision for image classification, is the only model that exhibits improved robustness on ImageNetV2. CLIP was trained on 400 million images with captions collected from various sources. For context, the ImageNet training set contains one million images [4]. Therefore it is possible that including CLIP into our set of models would reveal that ImageNetV2 and ImageNet are not $(0.31, 0.38, 0.005, 0.008)$ -close anymore. We note that there are multiple other models trained on larger datasets, but those models do not exhibit significant robustness with respect to ImageNetV2 [23].

In the third case, the new model is not similar to previous models. When this happens the new model can be above or below the line described by the previous models even when the two distributions are close. Our guess is that CLIP is not similar to previous models which makes effective robustness possible. We leave an analysis of CLIP to future work.

Several open questions remain. We offered sufficient conditions to guarantee that classifications models are approximately collinear, but it is not clear whether there are practical situations in which models are approximately collinear and our conditions are violated. Moreover, it is not clear when we can expect our conditions to hold. In particular, Assumption 1 is related to model similarity, but we do not understand why models are similar. Are models similar due to the training data, the model classes, or something else?

Acknowledgments. We thank Sara Fridovich-Keil, Benjamin Recht, Ludwig Schmidt, and Vaishaal Shankar for valuable feedback that helped us improve the clarity of the manuscript.

References

- [1] A. Barbu, D. Mayo, J. Alverio, W. Luo, C. Wang, D. Gutfreund, J. Tenenbaum, and B. Katz. Objectnet: A large-scale bias-controlled dataset for pushing the limits of object recognition models. In *Advances in Neural Information Processing Systems*, pages 9453–9463, 2019.
- [2] A. Ben-Tal, D. Den Hertog, A. De Waegenaere, B. Melenberg, and G. Rennen. Robust solutions of optimization problems affected by uncertain probabilities. *Management Science*, 59(2): 341–357, 2013.
- [3] E. Delage and Y. Ye. Distributionally robust optimization under moment uncertainty with application to data-driven problems. *Operations research*, 58(3):595–612, 2010.
- [4] J. Deng, W. Dong, R. Socher, L.-J. Li, K. Li, and L. Fei-Fei. ImageNet: A large-scale hierarchical image database. In *2009 IEEE conference on computer vision and pattern recognition*, pages 248–255. IEEE, 2009.
- [5] M. M. Deza and E. Deza. *Encyclopedia of Distances*. Springer, second edition, 2018.
- [6] J. C. Duchi, T. Hashimoto, and H. Namkoong. Distributionally robust losses against mixture covariate shifts. *arXiv:2007.13982*, 2020.
- [7] C. Dwork. Differential privacy. In *Proceedings of the International Colloquium on Automata, Languages and Programming (ICALP)*, pages 1–12, 2006.

- [8] C. Dwork, F. McSherry, K. Nissim, and A. Smith. Calibrating noise to sensitivity in private data analysis. In *Theory of cryptography conference*, pages 265–284. Springer, 2006.
- [9] C. Dwork, A. Roth, et al. The algorithmic foundations of differential privacy. *Foundations and Trends in Theoretical Computer Science*, 9(3-4):211–407, 2014.
- [10] P. M. Esfahani and D. Kuhn. Data-driven distributionally robust optimization using the Wasserstein metric: Performance guarantees and tractable reformulations. *Mathematical Programming*, 171(1-2):115–166, 2018.
- [11] D. Hendrycks, K. Zhao, S. Basart, J. Steinhardt, and D. Song. Natural adversarial examples. *arXiv preprint arXiv:1907.07174*, 2019.
- [12] S. Kpotufe and G. Martinet. Marginal singularity, and the benefits of labels in covariate-shift. In *Proceedings of the 31st Conference On Learning Theory*, volume 75 of *Proceedings of Machine Learning Research*, pages 1882–1886. PMLR, 2018.
- [13] A. Krizhevsky. Learning multiple layers of features from tiny images. 2009.
- [14] H. Mania, J. Miller, L. Schmidt, M. Hardt, and B. Recht. Model similarity mitigates test set overuse. In *Advances in Neural Information Processing Systems*, pages 9993–10002, 2019.
- [15] J. Miller, K. Krauth, B. Recht, and L. Schmidt. The effect of natural distribution shift on question answering models. In *Proceedings of the 37th International Conference on Machine Learning*, volume 119 of *Proceedings of Machine Learning Research*, pages 6905–6916. PMLR, 2020.
- [16] A. Radford, J. W. Kim, C. Hallacy, A. Ramesh, G. Goh, S. Agarwal, G. Sastry, A. Askell, P. Mishkin, J. Clark, et al. Learning transferable visual models from natural language supervision. *OpenAI*, 2021.
- [17] B. Recht, R. Roelofs, L. Schmidt, and V. Shankar. Do ImageNet classifiers generalize to ImageNet? In *Proceedings of the 36th International Conference on Machine Learning*, volume 97 of *Proceedings of Machine Learning Research*, pages 5389–5400. PMLR, 2019.
- [18] R. Roelofs, V. Shankar, B. Recht, S. Fridovich-Keil, M. Hardt, J. Miller, and L. Schmidt. A meta-analysis of overfitting in machine learning. In *Advances in Neural Information Processing Systems*, pages 9179–9189, 2019.
- [19] S. Sagawa, P. W. Koh, T. B. Hashimoto, and P. Liang. Distributionally robust neural networks for group shifts: On the importance of regularization for worst-case generalization. *arXiv preprint arXiv:1911.08731*, 2019.
- [20] S. Shafieezadeh Abadeh, P. M. Mohajerin Esfahani, and D. Kuhn. Distributionally robust logistic regression. *Advances in Neural Information Processing Systems*, 28:1576–1584, 2015.
- [21] V. Shankar, R. Roelofs, H. Mania, A. Fang, B. Recht, and L. Schmidt. Evaluating machine accuracy on ImageNet. In *Proceedings of the 37th International Conference on Machine Learning*, volume 119 of *Proceedings of Machine Learning Research*, pages 8634–8644. PMLR, 2020.

- [22] A. Sinha, H. Namkoong, R. Volpi, and J. Duchi. Certifying some distributional robustness with principled adversarial training. *International Conference on Learning Representations*, 2018.
- [23] R. Taori, A. Dave, V. Shankar, N. Carlini, B. Recht, and L. Schmidt. Measuring robustness to natural distribution shifts in image classification. In *Advances in Neural Information Processing Systems*, 2020.
- [24] C. Yadav and L. Bottou. Cold case: The lost MNIST digits. In *Advances in Neural Information Processing Systems*, pages 13443–13452, 2019.

A CIFAR-10.1 vs CIFAR-10

In this section we compare CIFAR-10.1 and CIFAR-10 in terms of $(\delta_1, \delta_2, \nu_1, \nu_2)$ -closeness based on 30 models collated by Recht et al. [17].

The blue points shown in Figure 6a represent probabilities of the 274,560 events defined by the triplets $\{f_i, f_j, f_k\}$, as considered in Definition 1. This empirical evaluation suggests that CIFAR-10 and CIFAR-10.1 satisfy our assumption with $\delta_1 = 0.0$, $\delta_2 = 1.7$, $\nu_1 = 0.005$, and $\nu_2 = 0.02$.

It is important to note that $\delta_2 = 1.7$ is a large value and if we were to plug it into (2) we would obtain a poor guarantee. However, we remark that the large slope is needed only for events whose probabilities according to CIFAR-10 are at most 0.03. For events with larger CIFAR-10 probabilities we could use a smaller δ_2 . For example, we could upper bound $\mathbb{Q}(A)$ using $\delta_2 = 0.8$ and $\nu_2 = 0.01$ for all events considered in Definition 1 that have $\mathbb{P}(A) \geq 0.03$. This choice would ensure that (1) are satisfied for over 95% of events. As explained in Section 4, our analysis can tolerate some violations of (1).

For convenience we reiterate our explanation here. Suppose we are given four models f_1, f_2, f_3, f_4 , and suppose (1) is satisfied by the events defined by (f_1, f_2, f_4) and (f_1, f_3, f_4) . Then, we can show that f_2 and f_3 lie close to the line defined by f_1 and f_4 , without needing the events defined by the triplets (f_1, f_2, f_3) and (f_2, f_3, f_4) to satisfy (1). Hence, we can guarantee that all models are approximately collinear even when some of the $6\binom{h}{3}$ events do not satisfy (1).

Moreover, we note that distribution closeness does not necessarily have to be defined in terms of linear upper and lower bounds, as in (1). Instead, our analysis can be performed with bounds of the form $-g_1(\mathbb{P}(A)) \leq \mathbb{Q}(A) - \mathbb{P}(A) \leq g_2(\mathbb{P}(A))$ for some nonnegative functions g_1 and g_2 . In other words, our analysis can be carried out whenever $|\mathbb{P}(A) - \mathbb{Q}(A)|$ is small for the events considered in Definition 1.

Figure 6b shows the dominance probabilities of all the pairs of CIFAR-10 models we considers. We note that all these probabilities are smaller than 0.08, with most of them being at most 0.04. Therefore, Assumption 1 is also satisfied with a small ζ .

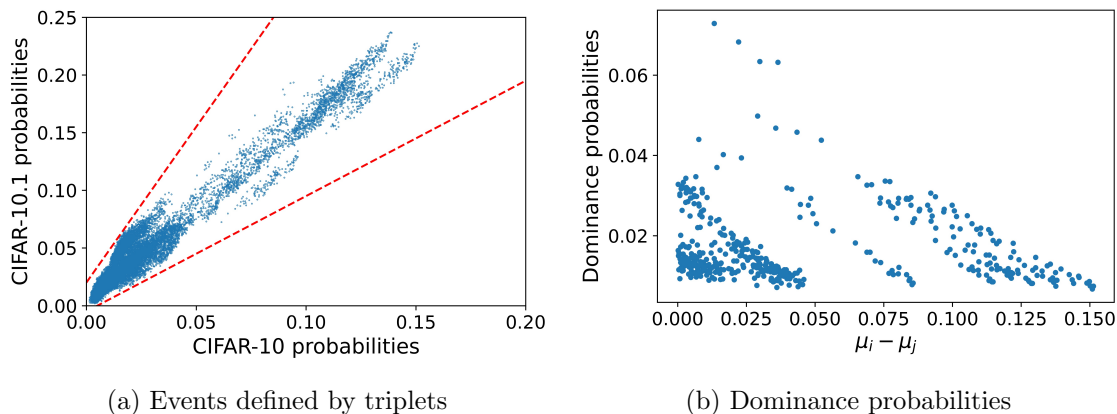


Figure 6: Figure 3b shows 24,360 blue points representing the probabilities of the events $A_i^{\varepsilon_i} \cap A_j^{\varepsilon_j} \cap A_k^{\varepsilon_k}$. The red dotted lines are upper and lower bounds on the probabilities under CIFAR-10.1, as in (1), with parameters: $\delta_1 = 0.0$, $\delta_2 = 1.7$, $\nu_1 = 0.005$, and $\nu_2 = 0.02$. Figure 3a shows the probabilities of the events $A_i^+ \cap A_j^-$ for all pairs of models with $\mu_i < \mu_j$ (i.e., the events on which a worse model is correct, but a better model is incorrect).

B Proof of Corollary 1

Let $A = (\mu_1, \tilde{\mu}_1)$ and $C = (\mu_h, \tilde{\mu}_h)$, and let $B = (\mu_i, \tilde{\mu}_i)$ be the point that has the largest residual from the line AC . Without loss of generality we assume that B is below or on the line AC . Then, there are two cases: all other models fall on or below the line AC , or there exists at least a point above the line AC .

The first case is immediately resolved by applying Proposition 1 to upper bound the residual r_B of B from the line AC . Then, we can choose ℓ to be the line that passes through the middle of the segments AB and BC . For this choice of ℓ the residual of any other point in our collection is upper bounded by $r_B/2$ because B has the largest residual and all other points lie on or below AC . The conclusion follows because the harmonic mean of two numbers with a constant sum is maximized when the two numbers are equal.

For the second case, let $D = (\mu_j, \tilde{\mu}_j)$ a point above the line AC with the largest residual from AC . We can assume that $\mu_1 < \mu_j < \mu_i$. Let r_B and r_D be B 's and D 's residuals from the line AC . By our extremal choices of B and D we know that if we consider the lines parallel to AC that pass through B and D respectively, we are guaranteed that all other points lie between them. Therefore, we can choose a line parallel to AC that has residual at most $(r_D + r_B)/2$ from all points.

Hence, we are left to upper bound r_B and r_D . From Proposition 1 we know that

$$r_B \leq \frac{2(\mu_h - \mu_i)(\mu_1 - \mu_i)}{\mu_h - \mu_1} \frac{\delta_1 + \delta_2}{2} + 3 \max\{\nu_1, \nu_2\}. \quad (7)$$

Since D is above the line AC , if we define by r'_D the residual from D to BC , we have $r_D \leq r'_D$. Then, from Proposition 1 we know that

$$r_D \leq r'_D \leq \frac{2(\mu_i - \mu_j)(\mu_j - \mu_1)}{\mu_i - \mu_1} \frac{\delta_1 + \delta_2}{2} + 3 \max\{\nu_1, \nu_2\}. \quad (8)$$

Let $c := \mu_j - \mu_1$, $b := \mu_i - \mu_j$, and $a := \mu_h - \mu_i$. Then, putting together (7) and (8) we find

$$r_B + r_D \leq \frac{2bc}{b+c} \frac{\delta_1 + \delta_2}{2} + \frac{2a(b+c)}{a+b+c} \frac{\delta_1 + \delta_2}{2} + 6 \max\{\nu_1, \nu_2\}.$$

Now, we would like to understand how large can the right hand side be as a function of just δ_1 , δ_2 , ν_1 , ν_2 , and $\mu_h - \mu_1$. In order to do this we find the maximum of the right hand side with respect to a , b , and c under the constraints $a, b, c \geq 0$ and $a + b + c = \mu_h - \mu_1$. Using simple first order conditions, one can find that

$$r_B + r_D \leq \frac{25}{32}(\mu_1 - \mu_h)\delta + 6 \max\{\nu_1, \nu_2\}.$$

The result follows by taking ℓ to be the line parallel to AC with equal residuals to B and D . We note that with a more involved proof it is possible to improve the constant $25/64$.

C The missing Fisher vector model

Recht et al. [17] collected and evaluated 67 models in their testbed. However, in the main text we chose to analyze only 66 of these models. In this section we explain our choice.

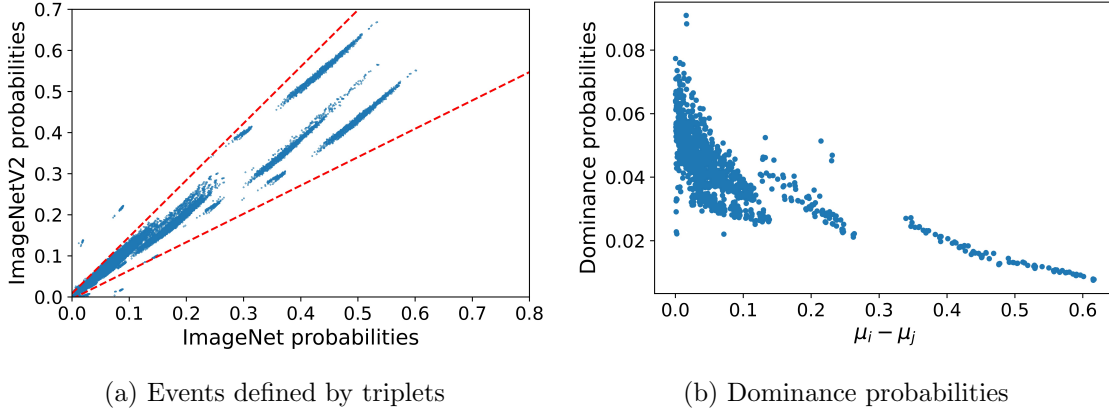


Figure 7: Figure 3b shows 287,430 blue points representing the probabilities of the events $A_i^{\varepsilon_i} \cap A_j^{\varepsilon_j} \cap A_k^{\varepsilon_k}$. The red dotted lines are upper and lower bounds, as in (1), with parameters: $\delta_1 = 0.31$, $\delta_2 = 0.38$, $\nu_1 = 0.005$, and $\nu_2 = 0.008$. Figure 3a shows the dominance probabilities for all pairs of 67 models.

Recht et al. [17] trained and implemented three Fisher vector models, with 16, 64, and 256 Gaussian Mixture Model centers. In our main analysis we removed the model that uses 64 GMM centers. We made this choice because leaving in this model would mislead one to think ImageNet and ImageNetV2 are far apart, as measured by Definition 1.

Figure 7a is a reproduction of Figure 3b with the missing Fisher vector included. We can see that now the wedge defined by $\delta_1 = 0.31$, $\delta_2 = 0.38$, $\nu_1 = 0.005$, $\nu_2 = 0.008$ does not include all the 287,430 events defined by the 67 models.

Since there are $\binom{66}{2} = 2145$ pairs of models that do not include the missing Fisher vector model and since each model triplet defines 6 relevant events, the missing Fisher vector model introduces 12,870 new points in Figure 3b compared to Figure 3b. However, just 666 of these events lie outside the wedge. Moreover, only 195 events are included in the three clusters that are far apart from the identity line, with the remaining points falling close to the origin.

As explained in Section 4 this kind of violation of 1 does not preclude our analysis. Also, the inclusion of the missing Fisher vector model does not violate Assumption 1, as can be seen from Figure 7b. Hence, for the sake of clarity we chose to omit the problematic Fisher vector model. Further investigation is needed to determine why this particular model defines events whose probabilities shift so much between ImageNet and ImageNetV2.